Examining Trends in Satellite-Detected Tropical Overshooting Tops as a Potential Predictor of Tropical Cyclone Rapid Intensification

SARAH A. MONETTE AND CHRISTOPHER S. VELDEN

Cooperative Institute for Meteorological Satellite Studies, University of Wisconsin—Madison, Madison, Wisconsin

KYLE S. GRIFFIN*

Department of Atmospheric and Environmental Sciences, University at Albany, State University of New York, Albany, New York

CHRISTOPHER M. ROZOFF

Cooperative Institute for Meteorological Satellite Studies, University of Wisconsin—Madison, Madison, Wisconsin

(Manuscript received 1 November 2011, in final form 12 June 2012)

ABSTRACT

A geostationary satellite–derived cloud product that is based on a tropical-overshooting-top (TOT) detection algorithm is described for applications over tropical oceans. TOTs are identified using a modified version of a midlatitude overshooting-top detection algorithm developed for severe-weather applications. The algorithm is applied to identify TOT activity associated with Atlantic Ocean tropical cyclones (TCs). The detected TOTs can serve as a proxy for ''hot towers,'' which represent intense convection with possible links to TC rapid intensification (RI). The purpose of this study is to describe the adaptation of the midlatitude overshooting-top detection algorithm to the tropics and to provide an initial exploration of possible correlations between TOT trends in developing TCs and subsequent RI. This is followed by a cursory examination of the TOT parameter's potential as a predictor of RI both on its own and in multiparameter RI forecast schemes. RI forecast skill potential is investigated by examining empirical thresholds of TOT activity and trends within prescribed radii of a large sample of developing North Atlantic TC centers. An independent test on Atlantic TCs in 2006–07 reveals that an empirically based TOT scheme has potential as a predictor for RI occurring in the subsequent 24 h, especially for RI maximum wind thresholds of 25 and 30 kt $(24\ \mathrm{h})^{-1}$ ($1\ \mathrm{kt} \approx 0.5\ \mathrm{m\ s^{-1}}$). As expected, the stand-alone TOT-based RI scheme is comparatively less accurate than existing objective multiparameter RI prediction methods. A preliminary experiment that adds TOT-based predictors to an objective logistic regression-based scheme is shown to improve slightly the forecast skill of RI, however.

1. Introduction

One of the essential ingredients to the intensification of tropical cyclones (TCs) is vigorous convection with associated latent-heat release through condensation processes (Adler and Rodgers 1977; Kuo 1965). Identifying and quantifying active convection in the tropics has been attempted in a variety of ways, mainly through the use of satellites (Steranka et al. 1986; Alcala and Dessler 2002; Liu and Zipser 2005; Romps and Kuang 2009; Olander and Velden 2009).

This paper examines a new geostationary satellite–based method that employs infrared window (IRW) imagery and an objective tropical-overshooting-top (TOT) detection algorithm in an effort to quantify vigorous tropical convection associated with TCs—in particular, prior to their rapid-intensification (RI) stages. The TOT detection algorithm is a modification of an existing overshooting-top (OT) algorithm that was originally developed for midlatitude severe-weather applications (Bedka et al. 2010, hereinafter B10). The OT detection criteria are retuned for use in the tropics in an attempt to identify the frequency and trends in TOTs during Atlantic Ocean TCs. Correlations between TOT

* Current affiliation: Department of Atmospheric and Oceanic Sciences, University of Wisconsin—Madison, Madison, Wisconsin.

Corresponding author address: Sarah A. Monette, Cooperative Institute for Meteorological Satellite Studies, 1225 W. Dayton St., Madison, WI 53706.
E-mail: sarah.monette@ssec.wisc.edu

DOI: 10.1175/JAMC-D-11-0230.1

© 2012 American Meteorological Society

trends and subsequent RI are then investigated to assess the utility of a TOT-based scheme as a possible tool for discrete and probabilistic forecasting of RI.

2. Algorithm description and datasets

a. TOT detection algorithm

The American Meteorological Society *Glossary of Meteorology* (Glickman 2000) defines an OT as "[a] domelike protrusion above a cumulonimbus anvil, representing the intrusion of an updraft through its equilibrium level." The definition of overshooting convection in the tropics varies, however. Previous research defined overshoots as convection that exceeds the height of the tropical tropopause (Montgomery and Farrell 1993; Simpson et al. 1998). Liu and Zipser (2005), however, suggest that the equilibrium level in the tropics which a TOT must exceed according to the *Glossary* definition is below the tropical tropopause. Therefore, although this algorithm is described as a TOT detection algorithm, it is important to note that no measure for evaluating the ambient height of the tropical tropopause has been included in the final modifications on the basis of the analysis from Liu and Zipser (2005).

The basic method of the objective OT detection algorithm (B10) is formulated around the premise that OTs appear as significantly colder IRW single pixels (or small clusters ≤15-km diameter) relative to their surrounding anvil-cloud mean temperature. Within the target scene of the IR image, the first step is to identify brightness temperature (BT) minima that are colder than 215 K. No BT minimum can be located within 15 km of another [Brunner et al. (2007) revealed that the largest detected OT diameters are ~12 km] so as to ensure that portions of the same OT are not classified as two independent overshoots.

The IRW BT of the anvil cloud surrounding a candidate OT is sampled at an 8-km radius (~2 pixels) from the coldest OT pixel in 16 directions (Fig. 1a). At this point, the B10 algorithm thresholds are modified for tropical convection applications. In the original B10 algorithm, at least five valid anvil pixels must have an IRW temperature at least as cold as 225 K for the candidate OT to be further considered. The pixels satisfying the 225-K criterion are used to calculate the mean anvil temperature, with the candidate OT classified as an OT if the minimum pixel BT and anvil-mean BT difference (BTD) is at least 6.5 K. In the modifications for tropical-cloud applications (mostly owing to a higher and colder tropopause), at least nine valid anvil pixels must satisfy the 225-K criterion and a candidate TOT is classified as a TOT if the BTD is at least 9 K. All of these threshold adjustments were determined empirically by testing combinations in forecast trials as described in section 4. A flow diagram that outlines the TOT detection algorithm scheme is shown in Fig. 1b.

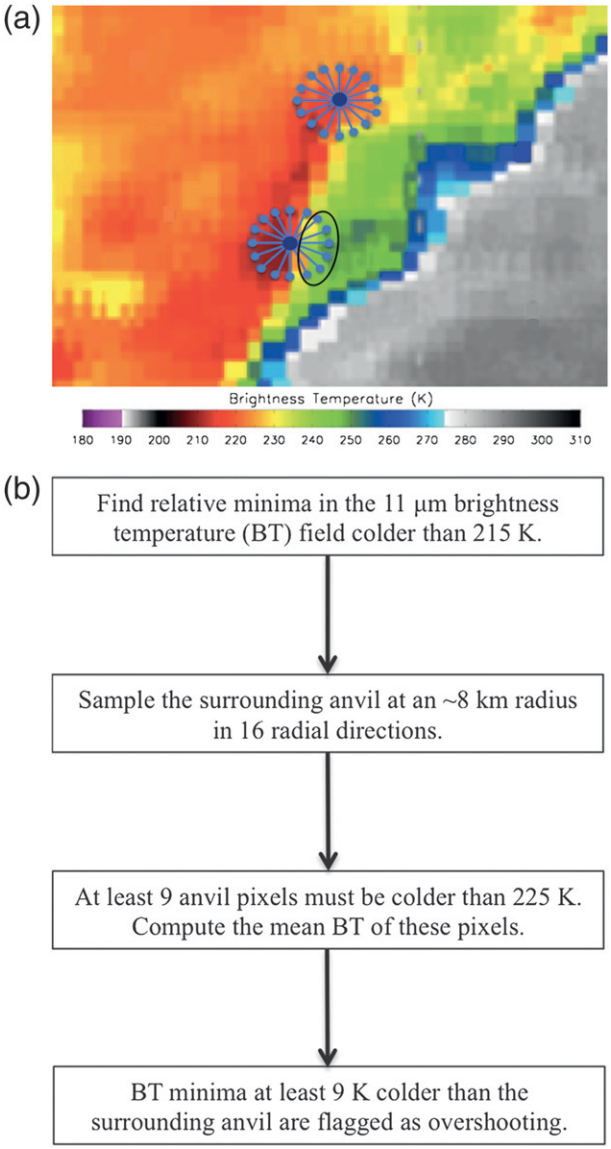

FIG. 1. (a) The process of identifying an overshooting top from 11-μm IR BTs. Local minima colder than 215 K are identified (dark-blue points), and the surrounding anvil is sampled in 16 radial directions at an 8-km radius (light-blue points). Candidate anvil pixels must have a BT colder than 225 K to be considered in the anvil temperature calculation. The black-circled pixels, which do not satisfy the criterion of BT ≤ 225-K, are not included in the mean anvil temperature calculation. At least 9 of the 16 anvil pixels must be valid and included in the mean anvil BT for the minimum to be classified as a candidate TOT. (b) A flow diagram describing the process of identifying an overshooting top using the TOT detection algorithm.

As a baseline, the TOT algorithm uses B10's 215-K threshold as the highest allowable BT to define a candidate TOT, even though the mean height of the tropical

tropopause is generally higher than that of midlatitudes. According to Jordan (1958), the temperature of the mean reference height for the equilibrium level [14.55 km, from Liu and Zipser (2005)] is approximately 205 K during the "hurricane season" of July–October. Although this is colder than the 215-K threshold used to define a candidate TOT, the geostationary satellite–analyzed cloud-top height when using the 4-km spatial resolution of the IRW is generally ~1 km lower than the estimated cloud-top heights using higher-spatial-resolution (1 km) visible imagery in deep tropical convection (Sherwood et al. 2004). This implies that the geostationary-satellite IRW-observed BT underestimates the actual TOT temperature by around 7–9 K, assuming a typical 7–9 K km^{-1} tropical lapse rate (Folkins 2002). Thus, the 215-K IRW cloud tops are actually representing ~208–206-K TOTs. In addition, the B10 215-K threshold is based on 1-km polar-orbiter IRW imagery, providing further motivation to keep the 215-K threshold as a baseline. Other (colder) thresholds are also explored in our search for optimum settings (section 4).

It will be shown in this study that the algorithm adapted to tropical applications is generally effective at detecting TOT trends, but there can be limitations in detecting individual convective events. In the original B10 OT detection algorithm, with a BTD of 6.5 K and removal of the numerical weather prediction estimated tropopause-temperature check, the OT probability of detection (POD) is around 90% when using the 1-km Moderate Resolution Imaging Spectroradiometer (MODIS) imagery correlated to *CloudSat*-observed OT events (Bedka et al. 2012). By comparison, our study, which employs geostationary satellite imagery with a spatial resolution of 3–4 km with a BTD setting of 9 K, finds only about one-half of that POD rate for TOTs as observed by *CloudSat*.

Reasons for undetected TOTs go beyond spatial-resolution issues (i.e., a TOT can be subpixel) and may include temporal sampling issues as well. Midlatitude OTs can have a life span as short as 10 min (Gettelman et al. 2002), allowing for the possibility of an OT (and therefore a TOT) to develop and decay from its peak between the normal 15-min image sampling by the geostationary satellite. A more problematic issue is that the TOT POD can be reduced in TCs with already established deep inner-core convection, which can diminish or completely mask the detection of TOT signatures, particularly from IR-based sensors. For example, Guimond et al. (2010) investigated the effects of convective hot towers (HTs) on the RI of Hurricane Dennis (2005). At 1453 UTC 9 July, an HT was identified near the eye of Dennis by an ER-2 aircraft Doppler radar (EDOP; see Fig. 2a). The IRW-detected TOTs at 1445 UTC (yellow points) and the path of the EDOP (white) are shown in Fig. 2b. In the region of the EDOP-detected HT, there was no TOT detected. As indicated in Fig. 2b, the area along the EDOP flight is approximately −70°C (203 K) in the IRW. This implies that the HT would need a BT of −79°C (194 K) or colder to be identified by the TOT detection algorithm. The HT has a BT of only −77°C (197 K), however. This is an example of a TC with an established cold central dense overcast from previous vigorous convection that hinders the satellite algorithm's ability to detect fresh TOTs that occur within it by reducing the BTD.

Despite these limitations, it will be shown that the detection algorithm can capture essential trends in TOT activity associated with most TCs. These trends will be examined for their correlation with TC RI in sections 3 and 4.

b. Satellite data

To cover the Atlantic hurricane development region, multiple geostationary satellite scans are employed in this study. The *Geostationary Operational Environmental Satellite-East* (*GOES-E*) scan of the contiguous United States (CONUS), with 15-min temporal resolution and 4-km spatial resolution, is utilized in a scan range from 110° to 62°W down to 15°N. Although greater temporal resolution is sometimes available with the CONUS rapid-scan schedule, these data are not utilized in our study because their use results in inconsistent TOT sampling during a portion of TC events. Beginning in 2004, Meteosat imagery, with a 3-km spatial resolution, also became available at 15-min temporal resolution and is used east of 55°W (the Meteosat images extend farther west, but the large viewing angle begins to affect TOT sampling beyond this range). TCs located between 55° and 62°W are analyzed with the *GOES-E* Northern Hemisphere (NH) scan, which also has 4-km spatial resolution but is limited to 30-min temporal resolution. For cases prior to 2004, TCs east of 62°W are analyzed by the *GOES-E* NH scan up to an easternmost extent of 40°W. TCs located west of 62°W but south of 15°N are also analyzed by the *GOES-E* NH scan. The various satellite scans are shown graphically in Fig. 3a for 1995–2003 cases and Fig. 3b for cases beginning in 2004.

c. Analysis periods, tracking, and validation

The data used in our investigation include 100 Atlantic TCs within the *GOES-E* CONUS viewing domain from 1995 to 2005 and 2008 that reach at least tropical-storm strength. In addition, nine TCs from 2004 to 2005 and 2008 whose entire track falls within the Meteosat scan are also analyzed, bringing the dependent sample

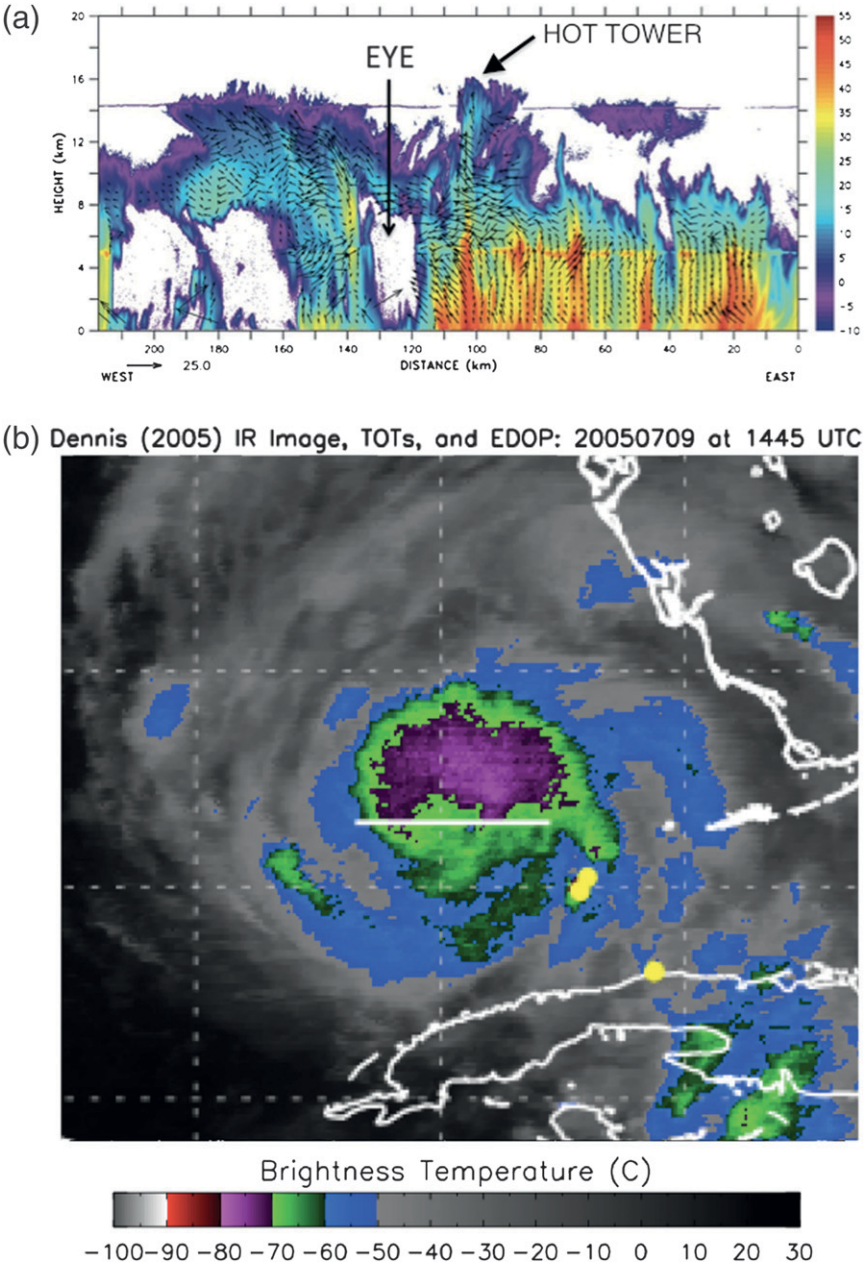

FIG. 2. (a) EDOP attenuation-corrected nadir-beam reflectivity at 1453 UTC 5 Jul 2005. An HT is located east of Dennis's eye. [The image is provided through the courtesy of Guimond et al. (2010).] (b) An IR image at 1445 UTC 5 Jul 2005, with the EDOP track (white) and detected TOTs (yellow dots to the southeast of the TC center) shown. No TOT is detected along the EDOP track because of effects arising from the very cold central dense overcast.

TC dataset to 109. A smaller subset consisting of all 23 Atlantic TCs from 2006 and 2007 is used in an independent test of performance. This independent test period was chosen to benchmark against the results of the operational rapid intensity index (RII) model presented by Kaplan et al. (2010, hereinafter KDK10). For validation, interpolated National Hurricane Center (NHC) best-track intensities (maximum 1-min sustained 10-m winds: MSW) are used, and RI is defined on the basis of three MSW thresholds: +25 kt (1 kt $\approx$ 0.5 m s^{-1}) in 24 h, which represent the 90th percentile of overwater 24-h TC intensity changes;

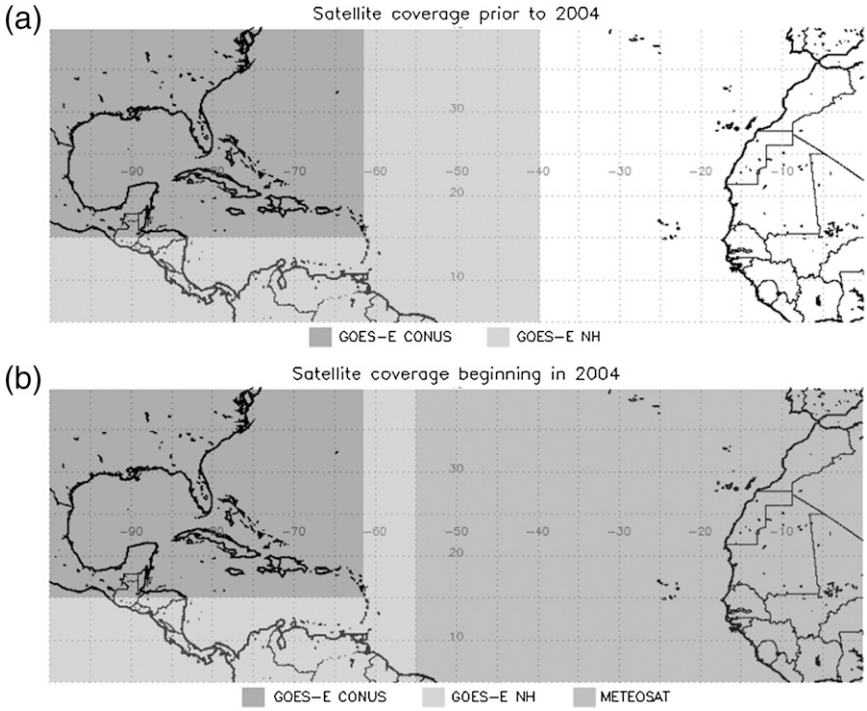

FIG. 3. (a) Satellite scan coverage for 1995–2003. Areas in dark gray have a 15-min temporal resolution with *GOES-E* CONUS, and areas in light gray have 30-min temporal resolution with *GOES-E* NH. GOES has a 4-km spatial resolution. (b) Satellite scan coverage beginning in 2004. Areas in dark (top-left part of panel) and medium (right part) gray have a 15-min temporal resolution with *GOES-E* CONUS and Meteosat, respectively. Areas in light gray have 30-min temporal resolution with *GOES-E* NH. GOES has a 4-km spatial resolution, and Meteosat has a 3-km spatial resolution.

+30 kt in 24 h (94th percentile); and +35 kt in 24 h (97th percentile) (KDK10).

Similar to procedures used in KDK10 and Rozoff and Kossin (2011, hereinafter RK11), cases in which the TC center is within 12 h of landfall or has reemerged over water in the previous 24 h are not analyzed. Cases are also not analyzed when the TC is of category-4 or category-5 intensity, because it is very uncommon for a TC of this strength to undergo RI (KDK10). Also, subtropical and extratropical cyclones and times when a system is categorized as an open wave are not analyzed (as determined from NHC best-track data).

3. Approach and method

We first take a cursory look at the use of TOT information as a predictor of RI to quickly assess the potential. To do this, we examine selected TCs and analyze time-averaged TOTs in increments of 1, 3, and 6 h prior to each synoptic time during the TC lifetime. These average TOTs per scan are then tabulated against the occurrence of RI or non-RI within the subsequent 24-h period. The difference between averages for RI and non-RI TOTs per scan must be significantly different at the 95% confidence level according to a two-sided Student's t test for the TOTs to be considered a viable predictor of RI (RK11). The results of this initial investigation are presented in section 4a.

Once the promising aspects of the TOTs as an RI predictor are established, we then examine TOT activity records for possible influences of non-RI-related signals. In particular, tropical convection has been found to have a diurnal signal (Hendon and Woodberry 1993). Using 11-μm BT data, Yang and Slingo (2001) found an early morning maximum in oceanic deep convection, with Kossin (2002) indicating an additional semidiurnal signal present in developed TCs. In an attempt to ameliorate these signals with respect to actual RI trends, we look at the TOTs averaged over 3-h periods. This time frame is chosen for analysis because the diurnal signal is less prevalent over a 3-h average than a 1-h average (Tory et al. 2006), and averaging over a 3-h window allows the diurnal and semidiurnal signals to present themselves without dominating the TOT signal. While

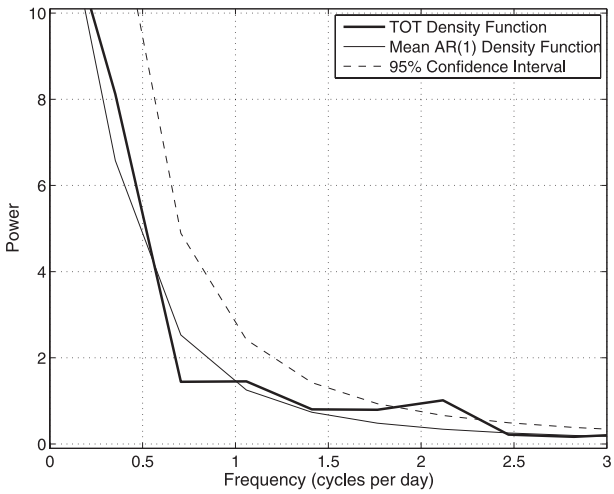

FIG. 4. Power spectrum from Hurricane Ike (2008). The thick solid line indicates the TOT density function for Ike. The thin solid line is the mean TOT density function for this TC, and the dashed line shows the 95% confidence about this mean. The TOT density function above the 95% confidence interval at 2 cycles per day signifies that a significant semidiurnal cycle signal may exist in this case.

averages longer than 3 h would continue to dampen the diurnal and semidiurnal signals, they could also significantly dampen shorter-term trends that are potentially indicative of RI.

A power spectral analysis is then conducted to help to reveal whether averaging the TOTs can negate the majority of the diurnal and semidiurnal signals. A first-order autoregression [AR(1)] process is used, which employs a single autoregressive parameter (in this case the correlation coefficient between two successive 3-h averages of TOTs per scan) to smooth over short-term variations while emphasizing the slower variations (Wilks 2006). A Hamming window, which adds one period of a cosine function to a rectangular window (Smith 2011a) at one-quarter of the average TOT time series length, rounded to the lowest integer, is also utilized. The power spectrum density, in cycles per day, is estimated using the Welch method (Smith 2011b).

An example of a semidiurnal signal from Hurricane Ike (2008) is shown in Fig. 4. The signal is indicated by the 3-h-averaged TOT density function that is greater than the 95% AR(1) confidence interval around 2 cycles per day. Only 19.8% of the TCs in our sample presented a semidiurnal signal, however, and only 3.1% exhibit a TOT density function that is greater than the AR(1) 95% confidence interval at 1 cycle per day (indicative of a diurnal signal). Thus, 3-h TOT averaging appears to dampen successfully the significant portion of the diurnal and semidiurnal signals found in our TC sample.

In the development of the TOT RI index, we also attempt to account for other sources of potential variance. One of the well-known inhibiting factors to intensity increases in a TC is vertical wind shear, which often presents itself through convective asymmetries. Furthermore, asymmetric temperature perturbations, which can be associated with the diluted TOT updrafts (Zipser 2003), have been found to have a negative effect on intensity (Nolan and Grasso 2003). Therefore, the index also considers the *distribution* of TOTs within the target area (defined as a prescribed radius from the TC center, as discussed in the next paragraph). To calculate the TOT distribution, the angle of each TOT (in degrees) from due north of the TC is calculated. The spread of the TOTs can then be observed by calculating the standard deviation of these angle degrees. If the standard deviation of the TOT angle degrees is less than or equal to 36°, and therefore 64.2% of the TOTs are within just one 20% sector of the TC near environment (assuming a normal distribution), the average TOTs per scan value for that analysis time is set to zero.

The next step in developing a TOT-based RI algorithm is to optimize TOT parameters/settings used in the index (spatial, temporal, BT intensity, and level of activity). To accomplish this optimization, we employ a large developmental dataset of Atlantic TCs from 1995 to 2005 and 2008. The analysis includes an examination of the following BT and BTD combinations: TOTs with a BT colder than 215, 205, or 200 K and a BTD of 9 K, as well as TOTs with a BT colder than 215 K and a BTD of 12 or 15 K. For each BT combination experiment, we examine five different radii from the TC center—all TOTs within 100, 150, 200, 300, and 500 km, and for each radius we analyze TOT averaging time frames of 3, 6, 12, and 24 h prior to each analysis time. Each BT–radii–time frame combination is then analyzed using preselected thresholds representing time averages of TOTs (i.e., number of TOTs per scan for the averaging time noted above, or ''average TOTs per scan''). These thresholds range from 0.5 to 6.5 TOTs per scan in increments of 0.5 TOTs per scan. A selection tree diagram illustrating this process is shown in Fig. 5.

The selection of an optimal combination of parameters and TOT threshold is then based on comparing their Peirce skill scores (PSS), with a PSS of 1 (0) representing a perfect (random) RI forecast (Wilks 2006). A forecast is deemed skillful if the PSS is greater than 0. The PSS is equal to the POD, the ratio of the correctly forecast RI occurrences to the actual number of RI occurrences, minus the probability of false detection (POFD), which is the number of false alarms divided by the total number of nonoccurrences. The false-alarm ratio (FAR) is

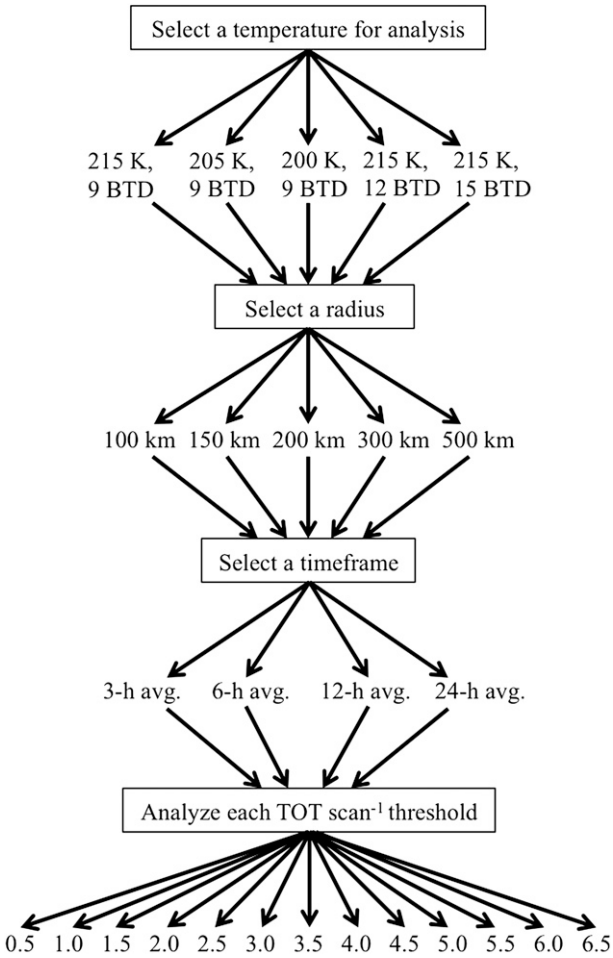

FIG. 5. A selection tree diagram illustrating the process used to identify the optimal temperature parameters, radii, time frame, and thresholds of average TOTs per scan for each RI threshold. This process results in 1300 different combination forecasts, which are analyzed for each RI threshold to identify the optimal parameters on the basis of the PSS.

calculated by dividing the number of incorrect forecasts of RI by the total number of RI forecasts. Both the POFD and FAR have negative orientations; thus, lower values are preferred. A 2 × 2 contingency table and equations for each metric can be found in Tables 1 and 2, respectively.

The TOT RI index approach to forecasting RI is similar to the operational RII, which forecasts the probability of RI at the synoptic hours of 0000, 0600, 1200, and 1800–UTC. The forecasts are validated using the 6-hourly NHC best-track 1-min maximum sustained 10-m wind values. Because the satellite imagery is available approximately every 15 min, however, the NHC best track is linearly interpolated to 15-min locations and intensities to coincide with the satellite scans.

TABLE 1. Relationship between TOT RI forecasts and observations in a 2 × 2 contingency table.

		Obs	
		Yes	No
Forecast	Yes	h	f
	No	m	z

It is prudently recognized that predicting RI relies on many environmental factors that cannot be accounted for simply by TOTs as a proxy for vigorous convection. Therefore, although the bulk of our study hopes to show the viability of TOTs as a *potential* predictor of RI, we recognize that the optimal way to include the information content in the TOT trends is through a multiparameter RI model. For example, a logistic regression scheme presented in RK11 attempts to objectively isolate predictors of RI, including those determined from geostationary satellites. This discriminative model fits coefficients for predictors obtained through an iterative least squares approach. Because the optimal logistic regression model predictors in RK11 are selected for 35-kt RI, this threshold is also used for the selection of optimal TOT predictors, which are added into the model as a preliminary assessment of the potential for RI forecast improvement.

4. Results

a. Proof of concept

As stated in the first paragraph of the previous section, the intent here is first to show whether the TOT RI index, as a stand-alone observable, has an identifiable relationship with RI. For a large sample of Atlantic TCs, we compare average TOTs per scan within specified radial disks from the storm center for cases of RI within the subsequent 24 h. Table 3 shows that TCs about to undergo RI have a greater number of TOT per scan than do those TCs that do not exhibit RI. From a two-sided Student's t test, the average number of TOTs per scan between cases in which RI occurs in the subsequent 24 h and non-RI cases is significantly different at the 99% confidence level (95% confidence interval for a 50-km radius).

TABLE 2. Forecast metrics for the TOT RI forecasts using the 2 × 2 contingency table in Table 1.

Forecast metric	Equation
PSS	$\frac{h}{h+m} - \frac{f}{f+z}$
POD	$h/(h+m)$
POFD	$f/(f+z)$
FAR	$f/(h+f)$

TABLE 3. Average TOTs per scan at selected radii r from the TC center in the 1, 3, and 6 h before synoptic time. Values are significantly different at the 99% confidence level except at a radius of 50 km, where the difference is significant at the 95% confidence level. TOTs are defined as at least 215 K with a BTD of at least 9 K. Results are shown for the 977 non-RI 24-h time frames and the 143 twenty-four-hour timeframes of verified 25-kt RI, the 1017 non-RI 24-h time frames and the 103 twenty-four-hour timeframes of verified 30-kt RI, and the 1032 non-RI 24-h timeframes and the 88 twenty-four-hour timeframes of verified 35-kt RI.

	r = 50 km	r = 100 km	r = 150 km	r = 200 km	r = 300 km	r = 500 km
			25-kt RI; N = 977/143			
TOTs (1 h)	0.10/0.19	0.34/0.57	0.65/1.03	1.08/1.66	2.17/3.10	3.94/5.45
TOTs (3 h)	0.10/0.16	0.33/0.48	0.64/0.91	1.04/1.47	2.04/3.00	3.69/5.34
TOTs (6 h)	0.12/0.15	0.33/0.47	0.64/0.91	1.04/1.50	2.07/2.99	3.77/5.30
			30-kt RI; N = 1017/103			
TOTs (1 h)	0.11/0.15	0.34/0.58	0.65/1.16	1.08/1.84	2.15/3.58	3.89/6.60
TOTs (3 h)	0.11/0.15	0.33/0.51	0.63/1.02	1.04/1.66	2.03/3.37	3.66/6.31
TOTs (6 h)	0.11/0.15	0.33/0.50	0.64/1.00	1.04/1.67	2.06/3.47	3.73/6.30
			35-kt RI; N = 1032/88			
TOTs (1 h)	0.11/0.19	0.34/0.70	0.63/1.40	1.06/2.25	2.11/4.34	3.81/7.90
TOTs (3 h)	0.11/0.17	0.32/0.59	0.63/1.18	1.02/1.97	2.01/4.01	3.59/7.51
TOTs (6 h)	0.12/0.18	0.33/0.56	0.63/1.15	1.02/1.97	2.03/4.04	3.67/7.42

This result provides the motivation to examine TOTs more carefully as a potential RI predictor. It also provides a place to start a more thorough investigation, in terms of TOT time averaging, spatial analysis (radial distances from the storm center), and TOT discrimination settings described in section 3. It is important to stress again that the TOTs by themselves do not represent the array of potential TC RI predictors, some of which are currently used by operational RI forecast guidance. The potential of TOTs as part of a multiparameter model RI predictor suite will be addressed in section 4d.

b. *Dependent dataset analysis*

1) RI: 25 KT IN 24 H

Analysis of the 1995–2005 and 2008 dependent dataset reveals the highest PSS for the TOT RI index is 0.356, with a POD of 60.9%, an FAR of 69.5%, and a POFD of 25.2%. The optimal parameters associated with this forecast are a 3-h average of 2.0 TOTs per scan at a TOT BT equal to or colder than 215 K with a BTD of 9 K within 300 km of the TC center. Thus, this forecast ignores the first 3 h of TOTs in the 6 h between synoptic times. The highest PSS for a forecast averaging 6 h of TOTs is 0.336, a 5.62% decrease.

2) RI: 30 KT IN 24 H

With a PSS of 0.408, the optimal thresholds for the TOT RI index are the same for 30-kt RI as for 25-kt RI: a 3-h average of 2.0 TOTs per scan at a TOT BT equal to or colder than 215 K, a BTD of 9 K, and within 300 km of the TC center. This forecast has a POD of 67.7%, which is higher than the POD for 25-kt RI. The FAR and POFD are also higher than those for 25-kt RI at 78.4% and 26.9%, respectively.

3) RI: 35 KT IN 24 H

For this RI category, the most accurate TOT RI index thresholds are the same as the most accurate 25- and 30-kt RIs: a 3-h average of 2.0 TOTs per scan at a TOT BT equal to or colder than 215 K, a BTD of 9 K, and within 300 km of the TC center and featuring a PSS equal to 0.383 with a POD of 67.0%, FAR of 86.9%, and POFD of 28.7%. It is notable that the optimal 25-, 30-, and 35-kt RI forecast settings are the same. While this consistency may be a good thing for forecasters, it also suggests that the TOT RI index has difficulty in distinguishing between forecast rates of RI.

c. *Independent dataset analysis*

Using the results from the dependent sample analysis described above, the TOT algorithm is tested as a predictor of 24-h RI on an independent sample of TCs from 2006 and 2007. The existing operational RII model performance can act as a benchmark in this analysis. The results from the TOT RI index and the RII for 25-kt RI are shown in Fig. 6. The TOT-based RI forecasts have a POD of 48.3%, with an FAR of 81.6% and a POFD of 24.5%. The resulting PSS of 0.238 is positive, indicating skill at predicting 25-kt RI. This skill is still below the RII benchmark, however, as seen by the lower PSS for the TOT RI index than for the RII. This is an expected result because of other important environmental factors being accounted for by the RII scheme. Another potential reason for the lower PSS, as previously described, is the variance infused by the effects from the TC central dense overcast becoming opaque (cold), especially prior

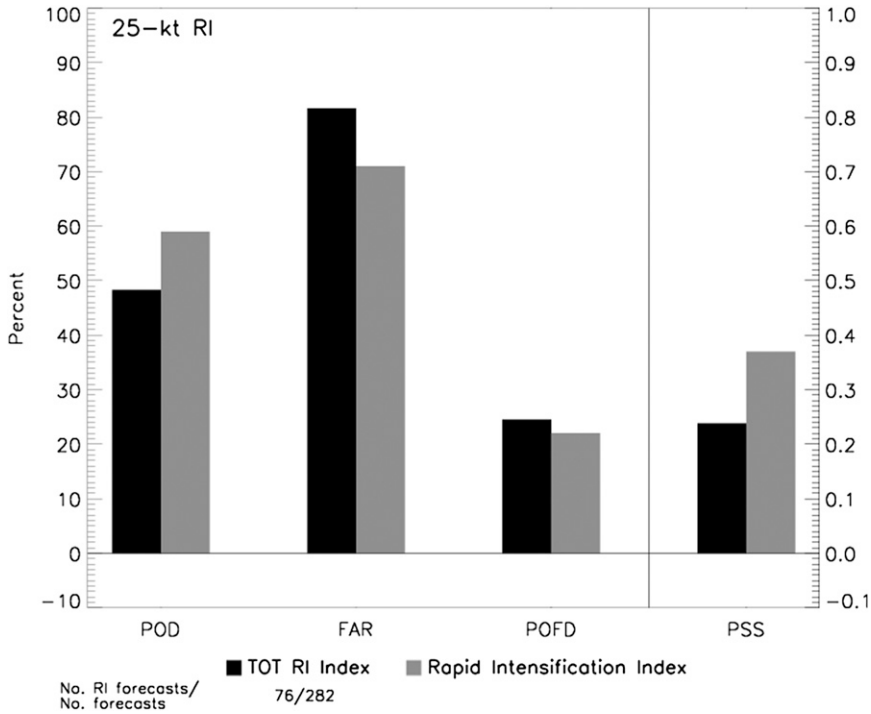

FIG. 6. POD, FAR, POFD, and PSS, for 25-kt RI using the TOT RI index forecast in comparison with the RII. The TOT RI index forecast is a 3-h average of 2.0 TOTs per scan with a BT of 215 K or colder and a BTD of greater than or equal to 9 K within 300 km of the TC center.

to and during RI, and thereby reducing the likelihood that potential new TOTs would survive the BTD thresholds with the surrounding anvil.

The independent dataset test has 62 false alarms, associated with 15 different TCs. Only two TCs are responsible for over half (35) of them: Florence and Helene from 2006. Ten false alarms from Florence occur during significant southwesterly wind shear (Beven 2007). During this time, an additional three RI forecasts were not made because of strong asymmetries in the detected TOTs. This is clearly a situation that would be better handled by a multiple-parameter RI scheme.

Figure 7 shows the results of forecasting 30-kt RI. Again, the TOT forecasts are skillful at predicting the occurrence of RI at this level, as defined by the positive PSS score of 0.206. The POD of 45.8% for the TOT RI index is comparable to the RII; the higher POFD (25.2%) for the TOT RI index results in a lower PSS when compared with the RII, however. The greater number of false alarms associated with the TOTs also results in a higher FAR (85.5%) than that for the RII (~70%).

Results for the 35-kt RI forecasts are shown in Fig. 8. With negative PSS scores, the TOT RI index does not show skill in predicting 35-kt RI on this limited sample.

Overall, the independent sample test shows that the TOT RI index has skill at predicting 25- and 30-kt RI as evidenced by the positive PSS, even though these forecasts are associated with relatively high FARs. This skill is less than that of the current RII from KDK10, however, which is an expected result given that other important environmental factors are being accounted for by the RII scheme.

d. TOTs as a predictor in a logistic regression model

While the previous results for stand-alone TOT-based indices confirm they are not as skillful at forecasting RI as the multiparameter RII, it has been shown that TOTs do have some correlation with RI and therefore potential as a predictor. The next logical step is to test whether the TOTs might have value in multiple-parameter RI schemes. As a preliminary assessment of this question, and before such a premise can be examined in the operational RII, we turn to the logistic regression scheme employed by RK11 to test potential forecast skill, which accounts for multiple synoptic predictors. The logistic regression approach objectively selects optimal TOT settings and, thus, can alter the thresholds from those found above.

By using the same 1995–2005 and 2008 dataset and case sample described above, TOT data are provided to the logistic regression algorithm at synoptic times.

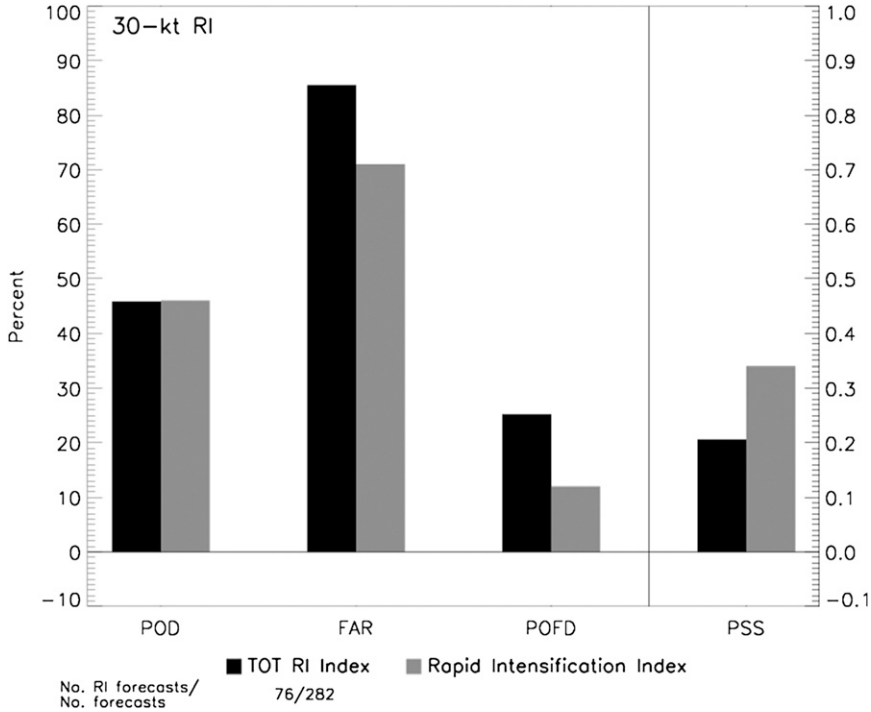

FIG. 7. As in Fig. 6, but for 30-kt RI.

Results indicate that the choices of TOT predictors are 3-h average TOTs within 50-km radius and 6-h average TOTs within 200 km of the TC center. These two TOT predictors are added to the seven predictors defined by Table 1 in RK11 for forecast skill verification. Although the original seven predictors include two from satellite-derived IRW, little correlation is found between these two predictors and the two TOT

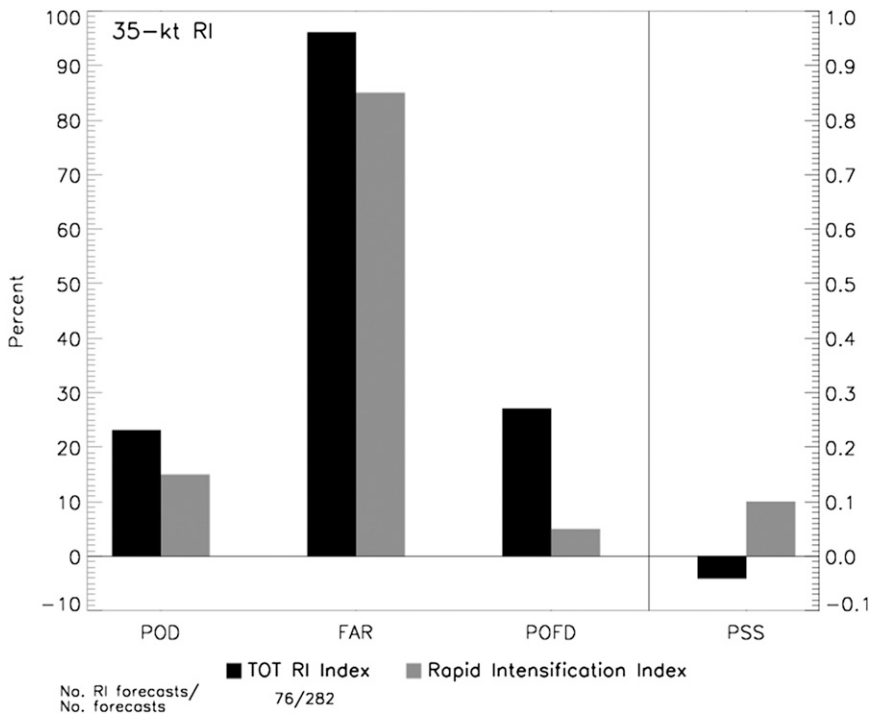

FIG. 8. As in Fig. 6, but for 35-kt RI.

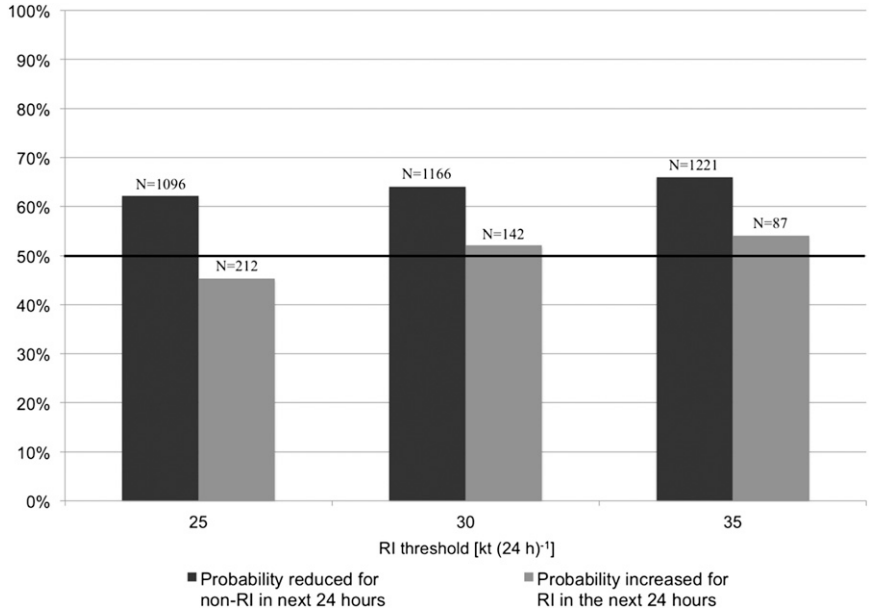

FIG. 9. Percent of improved forecasts when TOTs are added to the logistic regression model. TOTs reduce the probability of RI in 62% (25 kt), 64% (30 kt), and 66% (35 kt) of non-RI 24-h periods. TOTs increase the probability of RI in the next 24 h in 45% (25 kt), 52% (30 kt), and 54% (35 kt) of verifying cases.

predictors. Figure 9 shows the response of the calculated RI probability when including the TOTs. Overall, the results show that the addition of the TOT predictors is marginally effective at improving the prediction of RI in the next 24 h. The calculated probability for 25-kt RI that ''verifies'' is increased in only 45% of the cases, but that probability is increased in over 50% of the 30- and 35-kt RI cases. The addition of the TOT predictors also reduces the probability for RI forecasts in non-RI events, in all RI categories.

Figure 10 shows the results of the TOTs on the overall model forecast skill. The Brier skill scores (BSS) for the 25- and 35-kt RI forecasts increase by 3.2% and 1.6%, respectively, and the BSS for 30-kt RI does not significantly change (0.3% increase). Using this assessment metric, the addition of the TOT information has an overall small positive (but not statistically significant) impact on the forecast skill of the logistical regression scheme at predicting RI.

Reliability diagrams can often indicate where predictors have a positive contribution to the logistic regression scheme. In the reliability diagrams shown in Figs. 11a, 11c, and 11e, the 45° line represents perfect reliability for all forecast probabilities, with the horizontal and vertical dashed lines showing the climatological probability of RI. Points within the shaded region indicate forecast probabilities that contribute positively to the BSS, with points above the 45° line indicating forecast probabilities that are too low and points below the 45° line indicating forecast probabilities that are too high. For 25- and 30-kt RI forecasts (Figs. 11a and 11c, respectively), the addition of the TOTs produces a more reliable forecast at higher probabilities (≥0.5), with the exception of probabilities between 0.7 and 0.8. The results for 35-kt RI (Fig. 11e) are mixed, even though the logistic regression

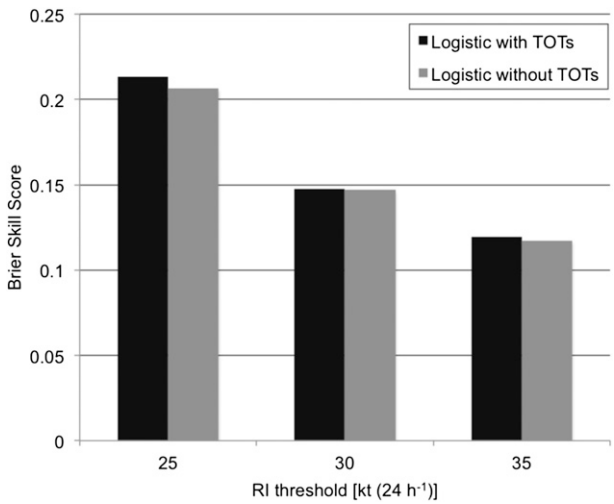

FIG. 10. BSSs for the logistic regression model presented by RK11 for the 132 TCs analyzed with TOTs predictors. An increase in the BSS represents improved forecast skill.

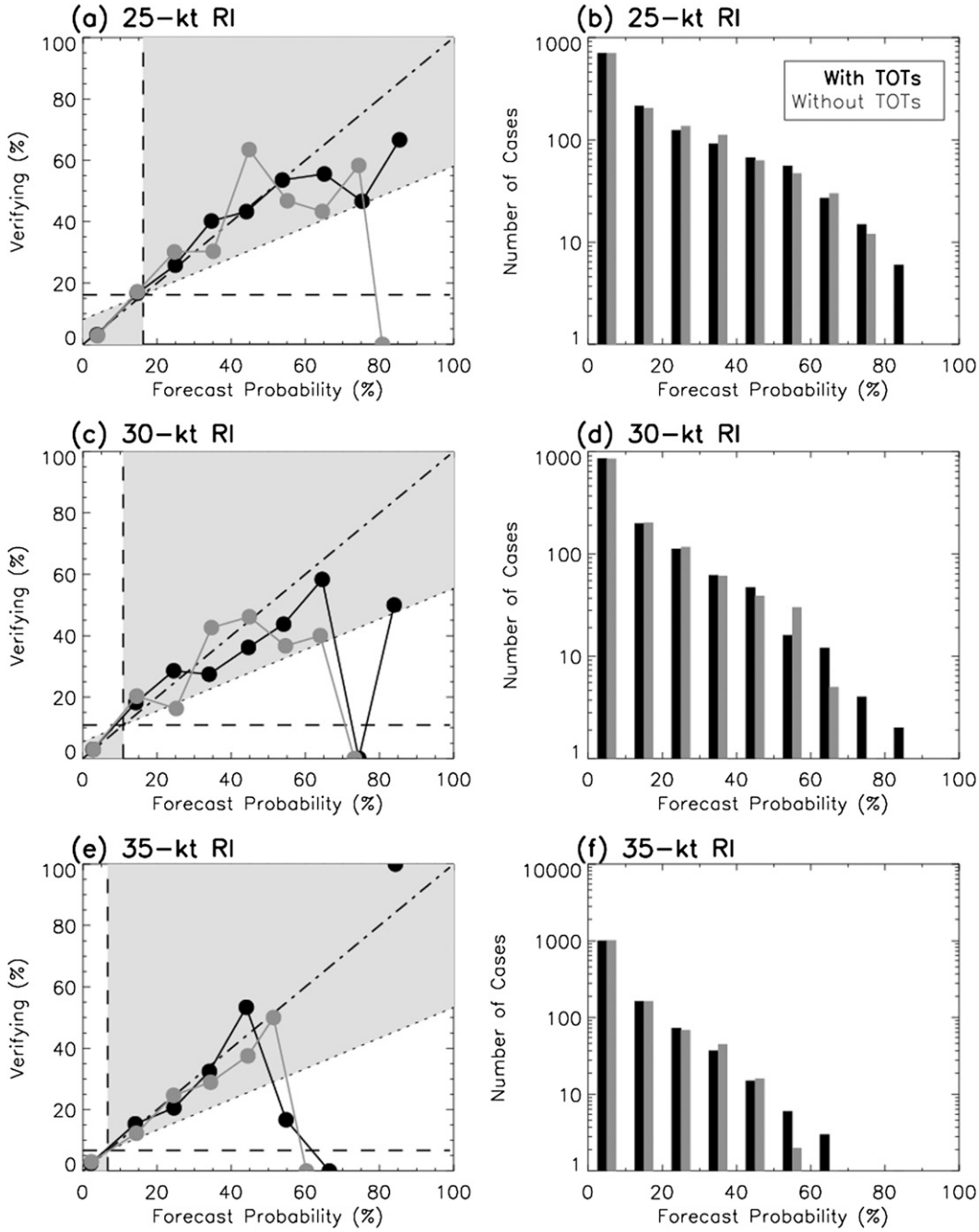

FIG. 11. Reliability diagrams from the logistic regression model with TOTs (black) and without TOTs (dark gray) for RI thresholds of (a) 25, (c) 30, and (e) 35 kt (24 h)$^{-1}$ and the corresponding number of forecasts for (b) 25, (d) 30, and (f) 35 kt (24 h)$^{-1}$ for probabilities of 0%–10%, 10%–20%, . . . , and 90%–100%.

scheme selected TOT predictors on the basis of this RI threshold.

It is again emphasized that the TOT information in this preliminary study was introduced into the model by a relatively simple selection scheme and may not represent the optimal approach. These results suggest that there is promise for the TOTs as a predictor in more sophisticated RI prediction models, and further exploration is warranted.

5. Summary and conclusions

This study applies an objective, satellite-based tropical-overshooting-top detection algorithm for identification

of intense tropical convection associated with Atlantic Ocean basin tropical cyclone rapid intensification. Using IR imagery from geostationary satellites, TOTs are identified using a modified algorithm that was originally designed for midlatitude thunderstorm development (Bedka et al. 2010). An empirical approach is used to optimize the algorithm settings for TC applications, such as spatial and temporal sampling and TOT brightness temperature thresholds. Once identified, different forecast approaches are tried to assess the potential of the TOT information to provide skill in predicting TC RI, either as a stand-alone algorithm or as input to multiparameter RI models (because RI is dependent on many environmental variables, some of which are not directly associated with TOT processes).

The results of our initial analysis show that, in general, trends in TOTs are correlated with RI, and the TOT activity between RI and non-RI cases differs at the 95% confidence level. Some specific findings are summarized as follows:

- An RI index that was developed on the basis of TOT activity is shown in independent sample testing to be skillful, as based on positive Peirce skill scores, at predicting the occurrence of 25- and 30-kt RI in the subsequent 24 h after analysis time, with a POD ranging from 23.1% to 48.3% and an FAR of 81.6%–96.1%. As expected, the performance of the stand-alone TOT-based RI algorithm is below that of the operational, multipredictor RI index but is promising enough to test the TOT information in a multiparameter model.
- As an initial experiment, TOT information is added to a multiparameter logistic regression model for RI prediction. The Brier skill score either increased slightly (25- and 35-kt RI) or remained constant (30-kt RI). The addition of the TOTs generally produces a more reliable forecast at higher probabilities ($\geq$0.5) for 25- and 30-kt RI, indicating the potential for further investigation of the TOTs as a situational predictor to add forecast improvement.

Overall, this study provides evidence that TOT activity can be correlated with TC RI. Just below one-half of the 25- and 30-kt RI cases and one-quarter of the 35-kt RI cases in our independent test sample were correctly predicted by just the stand-alone TOT indices, with positive Peirce skill scores indicating that the forecasts are skillful. These results demonstrate that increased TOT activity in TCs can be an indicator of imminent RI and should be further considered and tested as an input predictor to multiparameter RI forecast models.

Given the potential of TOT activity to indicate TC intensity behavior, the TOT products are being routinely derived in experimental mode over the Atlantic TC development region by the University of Wisconsin–Cooperative Institute for Meteorological Satellite Studies as part of the GOES-R Proving Ground project. As one of the new GOES products to be demonstrated during the hurricane season, analysts at the National Hurricane Center can access the products in near–real time to assess their potential utility in tropical analysis. In addition, the product is also being evaluated for general marine and aviation applications. Because the rapid-refresh 11-μm data from geostationary weather satellites are available for the tropics globally, the TOT products can be extended to and analyzed in other TC basins.

Acknowledgments. This research is funded by NOAA GOES-R Proving Ground Program Contract NA06NES4400002: Fund 144PH46 and NSF Grant AGS-0935830. The authors thank Kristopher Bedka (Science Systems and Applications, Inc.) for suggestions related to adapting his original OT detection algorithm to the tropics. Also, thanks are given to Lee Cronce, Justin Seiglaff, and Jason Brunner of the Cooperative Institute for Meteorological Satellite Studies for their assistance with running the TOT algorithm. We acknowledge Jason Dunion and two anonymous reviewers for very helpful comments that improved the manuscript.

REFERENCES

Adler, R. F., and E. B. Rodgers, 1977: Satellite-observed latent heat release in a tropical cyclone. *Mon. Wea. Rev.,* **105,** 956–963.

Alcala, C. M., and A. E. Dessler, 2002: Observations of deep convection in the tropics using the Tropical Rainfall Measuring Mission (TRMM) precipitation radar. *J. Geophys. Res.,* **107,** 4792, doi:10.1029/2002JD002457.

Bedka, K., J. Brunner, R. Dworak, W. Feltz, J. Otkin, and T. Greenwald, 2010: Objective satellite-based detection of overshooting tops using infrared window channel brightness temperature gradients. *J. Appl. Meteor. Climatol.,* **49,** 181–202.

——, R. Dworak, J. Brunner, and W. Feltz, 2012: Validation of satellite-based objective overshooting cloud-top detection methods using *CloudSat* cloud profiling radar observations. *J. Appl. Meteor. Climatol.,* **51,** 1811–1822.

Beven, J., 2007: Tropical cyclone report: Hurricane Florence (AL072006), 3–12 September 2006. National Hurricane Center Tropical Storm Rep. TCR-AL072006, 13 pp. [Available online at http://www.nhc.noaa.gov/pdf/TCR-AL072006_Florence.pdf.]

Brunner, J. C., S. A. Ackerman, A. S. Bachmeier, and R. M. Rabin, 2007: A quantitative analysis of the enhanced-V feature in relation to severe weather. *Wea. Forecasting,* **22,** 853–872.

Folkins, I., 2002: Origin of lapse rate changes in the upper tropical troposphere. *J. Atmos. Sci.,* **59,** 992–1005.

Gettelman, A., M. L. Salby, and F. Sassi, 2002: Distribution and influence of convection in the tropical tropopause region. *J. Geophys. Res.,* **110,** 4080, doi:10.1029/2001JD001048.

Glickman, T., Ed., 2000: *Glossary of Meteorology*. 2nd ed. Amer. Meteor. Soc., 855 pp.

Guimond, S. R., G. M. Heymsfield, and F. J. Turk, 2010: Multiscale observations of Hurricane Dennis (2005): The effects of hot towers on rapid intensification. *J. Atmos. Sci.,* **67,** 633–654.

Hendon, H. H., and K. Woodberry, 1993: The diurnal cycle of tropical convection. *J. Geophys. Res.,* **98,** 16 623–16 637.

Jordan, C. L., 1958: Mean soundings for the West Indies area. *J. Meteor.,* **15,** 91–97.

Kaplan, J., M. DeMaria, and J. A. Knaff, 2010: A revised tropical cyclone rapid intensification index for the Atlantic and eastern North Pacific basins. *Wea. Forecasting,* **25,** 220–241.

Kossin, J. P., 2002: Daily hurricane variability inferred from GOES infrared imagery. *Mon. Wea. Rev.,* **130,** 2260–2270.

Kuo, H. L., 1965: On formation and intensification of tropical cyclones through latent heat release by cumulus convection. *J. Atmos. Sci.,* **22,** 40–63.

Liu, C., and E. J. Zipser, 2005: Global distribution of convection penetrating the tropical tropopause. *J. Geophys. Res.,* **110,** D23104, doi:10.1029/2005JD006063.

Montgomery, M. T., and B. F. Farrell, 1993: Tropical cyclone formation. *J. Atmos. Sci.,* **50,** 285–310.

Nolan, D. S., and L. D. Grasso, 2003: Nonhydrostatic, three-dimensional perturbations to balanced, hurricane-like vortices. Part II: Symmetric response and nonlinear simulations. *J. Atmos. Sci.,* **60,** 2076–2087.

Olander, T. L., and C. S. Velden, 2009: Tropical cyclone convection and intensity analysis using differenced infrared and water vapor imagery. *Wea. Forecasting,* **24,** 1558–1572.

Romps, D. M., and Z. Kuang, 2009: Overshooting convection in tropical cyclones. *Geophys. Res. Lett.,* **36,** L0984, doi:10.1029/2009GL037396.

Rozoff, C. M., and J. P. Kossin, 2011: New probabilistic forecast models for the prediction of tropical cyclone rapid intensification. *Wea. Forecasting,* **26,** 677–689.

Sherwood, S. C., J.-H. Chae, P. Minnis, and M. McGill, 2004: Underestimation of deep convective cloud tops by thermal imagery. *J. Geophys. Res.,* **31,** L11102, doi:10.1029/2004GL019699.

Simpson, J., J. B. Halverson, B. A. Ferrier, W. A. Peterson, R. H. Simpson, R. Blackeslee, and S. L. Durden, 1998: On the role of ''hot towers'' in tropical cyclone formation. *Meteor. Atmos. Phys.,* **67,** 15–35.

Smith, J. O., III, cited 2011a: Spectral audio signal processing: generalized Hamming window family. [Available online at https://ccrma.stanford.edu/~jos/sasp/Generalized_Hamming Window_Family.html#eq:ghwf.]

——, cited 2011b: Welch's method. [Available online at https://ccrma.stanford.edu/~jos/sasp/Welch_s_Method.html.]

Steranka, J., E. B. Rodgers, and R. C. Gentry, 1986: The relationship between satellite measured convective bursts and tropical cyclone intensification. *Mon. Wea. Rev.,* **114,** 1539–1546.

Tory, K. J., M. T. Montgomery, and N. E. Davidson, 2006: Prediction and diagnosis of tropical cyclone formation in an NWP system. Part I: The critical role of vortex enhancement in deep convection. *J. Atmos. Sci.,* **63,** 3077–3090.

Wilks, D. S., 2006: *Statistical Methods in the Atmospheric Sciences*. 2nd ed. Academic Press, 627 pp.

Yang, G.-Y., and J. Slingo, 2001: The diurnal cycle in the tropics. *Mon. Wea. Rev.,* **129,** 784–801.

Zipser, E. J., 2003: Some views on ''hot towers''after 50 years of tropical field programs and two years of TRMM data. *Cloud Systems, Hurricanes, and the Tropical Rainfall Measuring Mission (TRMM), Meteor. Monogr.,* No. 51, Amer. Meteor. Soc., 49–58.